

Forward–Backward Semiclassical Dynamics with Information-Guided Noise Reduction for a Molecule in Solution[†]

Edward Bukhman and Nancy Makri*

Department of Chemistry, University of Illinois, 601 South Goodwin Avenue, Urbana, Illinois 61801.

Received: March 19, 2007; In Final Form: May 3, 2007

The forward–backward semiclassical dynamics (FBSD) methodology is used to obtain expressions for time correlation functions of a system (atom or molecule) in solution. We use information-guided noise reduction (IGNoR) [Makri, *N. Chem. Phys. Lett.* **2004**, *400*, 446] to minimize the statistical error associated with the Monte Carlo integration of oscillatory functions. This is possible by reformulating the correlation function in terms of an oscillatory solvent-dependent contribution whose integral can be obtained analytically and a slowly varying function obtained via a grid-based iterative evaluation of solute properties. Knowledge of the exact integral of the oscillatory function, combined with correlated statistics, leads to partial cancellation of the Monte Carlo error. Application on a one-dimensional solute–solvent model shows a substantial improvement of convergence in the IGNU-enhanced FBSD correlation function for a fixed number of Monte Carlo samples. The reduction of statistical error achieved by using the IGNU methodology becomes more significant as the number of solvent particles increases.

I. Introduction

In a series of papers,^{1–19} our group has described and applied an efficient methodology for simulating the dynamics of polyatomic systems under conditions where the latter exhibit substantial deviations from classical behavior, while decoherence quenches any quantum interference effects characteristic of low-dimensional Hamiltonians. This methodology employs a fully quantum mechanical path integral representation of the Boltzmann operator, along with a classical trajectory description of the dynamics obtained from the stationary phase limit of the exact expression for the time-dependent function of interest (e.g., time correlation function or expectation value).

Several semiclassical formulations of time correlation functions are available. The most rigorous (and accurate) semiclassical approach consists of applying the semiclassical approximation (either in the coordinate²⁰ or in a phase space²¹ representation) to each of the two time evolution operators that enter a time correlation function.^{22–29} By retaining the full semiclassical phase, such double semiclassical expressions usually offer a faithful description of quantum mechanical effects, including interference. At the same time, the presence of the semiclassical phase leads to severe instabilities in the Monte Carlo evaluation of such functions, which becomes impractical for many-particle systems. The so-called “sign problem” is circumvented in formulations that eliminate (partially or entirely) the oscillatory semiclassical phase. Partial elimination of the phase is possible through initial value representations with a momentum jump at the end of the forward trajectory³⁰ or generalized forward–backward procedures;³¹ these methods can capture quantum phase interference effects. Total elimination of the semiclassical phase leads to expressions that converge with much less computational effort. These include the well-known Wigner form^{32,33} (also derived via a linearized semiclassical treatment,^{34–37} and forward–backward schemes.^{1–19,31,38–45}

The forward–backward semiclassical dynamics (FBSD) methodology developed in our group is obtained by using a derivative identity to convert one of the two probed operators in the correlation function into an exponential form and applying the semiclassical approximation in a coherent state representation to the resulting product of three evolution-like operators. FBSD expressions are similar (and, within the stationary phase approximation, equivalent) to those of the Wigner formalism, but the phase space density of the former is directly amenable to fully quantum mechanical path integral treatments. (Evaluation of the Wigner function requires a Fourier-like transformation of the density operator, which, in the past, has been feasible only within locally harmonic^{46,47} or imaginary-time Gaussian^{48–51} approximations.) A number of applications^{10,12,15,16,52} have shown that FBSD provides a faithful representation of the short-time dynamics of fluids that exhibit substantial or even qualitative deviations from classical behavior, even in the superfluid phase.

FBSD expressions contain a phase space density, obtained through a coherent state transformation of the density operator (the Boltzmann operator for systems at finite temperature). Evaluation of the latter via the path integral representation results in an integrand with a small oscillatory component. Even though the small negative amplitude regions occur only in the wings of the phase space distribution, phase cancellation can become a serious issue in calculations with hundreds of degrees of freedom. This is so because small negative portions multiply positive regions, and the volume of negative parts approaches the volume of positive parts at an exponential rate as the number of particles is increased.⁵³ For this reason, FBSD calculations converge slower than purely classical phase space averages, often requiring millions of trajectories for acceptable precision. Thus, devising techniques that enhance the convergence of these calculations is highly desirable. Further, recent applications of FBSD focused on various neat fluids, where one can average the computed observable properties with respect to all the particles in the simulation, leading to a

[†] Part of the “Thom H. Dunning, Jr. Festschrift”.

* Corresponding author.

significant enhancement of the statistics. The simulation of a molecule in solution, however, where the statistics cannot benefit from a similar averaging, is expected to be significantly more challenging.

The present paper presents our recent progress in using FBSD ideas to simulate dynamical properties for a particle in solution. Makri recently introduced information-guided noise reduction⁵⁴ (IGNoR), a methodology for improving the statistics in Monte Carlo calculations of oscillatory integrals. This applies to situations where the integrand is a product of an oscillatory function whose integral is known and a slowly varying function. The main idea is that knowledge of the exact integral of the oscillatory function constrains the positive and negative volumes, such that only one of the two needs to be calculated by Monte Carlo sampling. Taking advantage of correlations, IGNoR obtains the desired integral by calculating how much the slowly varying function modifies the positive and negative volumes of the oscillatory function. In high-dimension space, where smooth functions tend to affect the positive and negative regions of the integrand in very similar ways, one can show that the application of IGNoR can lead to a dramatic reduction in the statistical error.

The methodology is described in section II. After a short review of the FBSD methodology, this section applies FBSD to a particle in solution, focusing in particular on the momentum autocorrelation function of the solute. Next, the integrand is split into two parts, and each of the two is evaluated by IGNoR procedures. In section III we demonstrate the benefits of the IGNoR-enhanced FBSD methodology by applying it to a one-dimensional solute–solvent model. Finally, some concluding remarks are given in section IV.

II. Methodology

The need for semiclassical descriptions arises because dynamical properties are sought that are too difficult to obtain with a fully quantum mechanical description. In the FBSD approximation, particles obey classical mechanics, but the trajectories are weighted by the Boltzmann factors of the initial quantum mechanical description of the system. As long as quantum interference effects are naturally suppressed by decoherence, this methodology enjoys considerable accuracy and scaling advantages over classical molecular dynamics and fully quantum mechanical approaches, respectively.

A. FBSD Expressions. One commonly evaluated time-dependent object is the correlation function of a particle. Time correlation functions have the following general form:

$$C_{AB}(t) = \frac{1}{Z} \text{Tr}(e^{-\beta\hat{H}} \hat{A} e^{i\hat{H}t/\hbar} \hat{B} e^{-i\hat{H}t/\hbar}) \quad (2.1)$$

Here \hat{H} is the Hamiltonian of a d -particle system, \hat{A} and \hat{B} are arbitrary operators, and Z is the canonical partition function. Here \hat{A} operates on the initial state of system, while $\hat{B}(t) = e^{i\hat{H}t/\hbar} \hat{B} e^{-i\hat{H}t/\hbar}$ operates on the system at a later time. In the derivative version of FBSD developed by our group,⁴ the operator \hat{B} is expressed as a product of exponentials according to the following identity:

$$\hat{B}(t) = -i \frac{\partial}{\partial \mu} e^{i\hat{H}t/\hbar} e^{i\mu\hat{B}} e^{-i\hat{H}t/\hbar} \Big|_{\mu=0} \quad (2.2)$$

Application of the forward–backward semiclassical approximation in a coherent state representation²¹ leads to the following

FBSD form for the operator:⁵⁵

$$\hat{B}(t) = \frac{1}{(2\pi\hbar)^{3d}} \int d\mathbf{q}_0 \int d\mathbf{p}_0 B(\mathbf{q}, \mathbf{p}_t) \times \left[\left(1 + \frac{3}{2}d\right) \langle \mathbf{q}_0 \mathbf{p}_0 | \langle \mathbf{q}_0 \mathbf{p}_0 | - 2\gamma \cdot (\hat{\mathbf{q}} - \mathbf{q}_0) | \mathbf{q}_0 \mathbf{p}_0 \rangle \langle \mathbf{q}_0 \mathbf{p}_0 | (\hat{\mathbf{q}} - \mathbf{q}_0) \right] \quad (2.3)$$

Here \mathbf{q}_0 and \mathbf{p}_0 are the d -dimensional vectors of the initial phase space variables, which serve as the initial conditions for classical trajectories that evolve according to Hamilton's equations of motion, $|\mathbf{q}_0 \mathbf{p}_0\rangle$ are the coherent state functions of the form

$$\langle \mathbf{q} | \mathbf{q}_0 \mathbf{p}_0 \rangle = \left(\frac{2}{\pi}\right)^{3d/4} (\det \gamma)^{1/4} \times \exp\left[-(\mathbf{q} - \mathbf{q}_0) \cdot \gamma \cdot (\mathbf{q} - \mathbf{q}_0) + \frac{i}{\hbar} \mathbf{p}_0 \cdot (\mathbf{q} - \mathbf{q}_0)\right] \quad (2.4)$$

and γ is a diagonal matrix of coherent state width parameters. Substitution in eq 2.1 yields the following FBSD expression for the correlation function:

$$C_{AB}(t) = (2\pi\hbar)^{-3d} Z^{-1} \int d\mathbf{q}_0 \int d\mathbf{p}_0 B(\mathbf{q}(t), \mathbf{p}(t)) \times \left[\left(1 + \frac{3}{2}d\right) \langle \mathbf{q}_0 \mathbf{p}_0 | e^{-\beta\hat{H}} \hat{A} | \mathbf{q}_0 \mathbf{p}_0 \rangle - 2\langle \mathbf{q}_0 \mathbf{p}_0 | (\hat{\mathbf{q}} - \mathbf{q}_0) \cdot e^{-\beta\hat{H}} \hat{A} \gamma \cdot (\hat{\mathbf{q}} - \mathbf{q}_0) | \mathbf{q}_0 \mathbf{p}_0 \rangle \right] \quad (2.5)$$

The FBSD procedure can also be applied to obtain an expression for the inner product of two vector operators. In that case, the FBSD expression takes the form¹¹

$$C_{A \cdot B}(t) = Z^{-1} \text{Tr}(e^{-\beta\hat{H}} \hat{A}(0) \cdot \hat{B}(t)) = (2\pi\hbar)^{-3d} Z^{-1} \int d\mathbf{q}_0 \int d\mathbf{p}_0 \left(1 + \frac{3}{2}d\right) \langle \mathbf{q}_0 \mathbf{p}_0 | e^{-\beta\hat{H}} \hat{A} | \mathbf{q}_0 \mathbf{p}_0 \rangle \cdot \mathbf{B}(\mathbf{q}(t), \mathbf{p}(t)) - 2(2\pi\hbar)^{-3d} Z^{-1} \int d\mathbf{q}_0 \times \int d\mathbf{p}_0 \langle \mathbf{q}_0 \mathbf{p}_0 | (\hat{\mathbf{q}} - \mathbf{q}_0) \cdot e^{-\beta\hat{H}} [\hat{A} \cdot \mathbf{B}(\mathbf{q}(t), \mathbf{p}(t))] \cdot \gamma \cdot (\hat{\mathbf{q}} - \mathbf{q}_0) | \mathbf{q}_0 \mathbf{p}_0 \rangle \quad (2.6)$$

The Boltzmann operator in these expressions is evaluated using the conventional path integral discretization. Due to the presence of coherent states, the resulting expression differs from the common path integral representation of the partition function in terms of position states in that the resulting “necklace”⁵⁶ now closes on a special phase space “bead” that specifies the starting point of a classical trajectory. For sufficiently short imaginary time steps $\Delta\beta = \beta/N$, the propagator can be written in the approximate form

$$\langle \mathbf{q}' | e^{-\Delta\beta\hat{H}} | \mathbf{q}'' \rangle = \langle \mathbf{q}' | e^{-\Delta\beta\hat{T}} | \mathbf{q}'' \rangle e^{-1/2\Delta\beta[V(\mathbf{q}') + V(\mathbf{q}'')]} \quad (2.7)$$

This approximation arises directly from the well-known Trotter splitting of the total Hamiltonian into kinetic and potential energy. (However, we note that the more accurate pair–product approximation,⁵⁷ also available in the coherent state form,¹² can be cast in a similar form by replacing the average potential by an effective two-particle potential that depends on the coordinates of both endpoints. To simplify the presentation, we retain the form of eq 2.7, noting it is a straightforward matter to implement the procedure described below with the pair–product form.) By implementing the discretized path integral treatment of the Boltzmann operator,⁵⁸ it has been shown that the integrand of eq 2.6 consists of an exponential part Θ that arises from the

discretized Boltzmann operator and a non-exponential part $\Lambda_{\mathbf{A}, \mathbf{B}}$ that includes all time-dependent contributions:

$$C_{\mathbf{A}, \mathbf{B}}(t) = (2\pi\hbar)^{-3d} \int d\mathbf{q}_0 \int d\mathbf{p}_0 \times \int d\mathbf{q}_1 \cdots \int d\mathbf{q}_N \Theta(\mathbf{q}_0, \mathbf{p}_0, \mathbf{q}_1, \dots, \mathbf{q}_N) \Lambda_{\mathbf{A}, \mathbf{B}}(\mathbf{q}_0, \mathbf{p}_0, \mathbf{q}_1, \dots, \mathbf{q}_N) \quad (2.8)$$

The function

$$\Theta(\mathbf{q}_0, \mathbf{p}_0, \mathbf{q}_1, \dots, \mathbf{q}_N) = (2\pi\hbar)^{-3d} \langle \mathbf{q}_0, \mathbf{p}_0 | e^{-\Delta\beta\hat{H}_0/2} | \mathbf{q}_1 \rangle e^{-\Delta\beta V(\mathbf{q}_1)} \times \langle \mathbf{q}_1 | e^{-\Delta\beta\hat{H}_0} | \mathbf{q}_2 \rangle \cdots \times e^{-\Delta\beta V(\mathbf{q}_N)} \langle \mathbf{q}_N | e^{-\Delta\beta\hat{H}_0/2} | \mathbf{q}_0, \mathbf{p}_0 \rangle \quad (2.9)$$

is the integrand of the partition function in the coherent state representation, and $\Lambda_{\mathbf{A}, \mathbf{B}}$ has been given in previous publications^{11,15} for specific forms of the probed operators.

Unlike the purely classical form of a correlation function, the FBSD expressions contain (for $N > 1$) oscillatory phase factors. Because the statistical error in Monte Carlo calculations grows exponentially with integral dimension when the integrand appears to be even mildly oscillatory when viewed in the space of a single integration variable,⁵³ numerical evaluation of FBSD correlation functions can be demanding. Nevertheless, these slow oscillations occur in the wings of the distribution where the density is small. If, in addition, the property of interest is averaged with respect to all the particles, as in the case of a correlation function in a neat fluid, convergence is reached with modest amounts of effort. Recent work in our group has demonstrated that momentum correlation functions can be evaluated with adequate efficiency in liquids where $\sim 10^2$ atoms are treated explicitly.

B. FBSD for a Molecule in Solution. The focus of this paper is on the correlation function of a system (atom or molecule) in solution, where $\hat{\mathbf{A}}$ and $\hat{\mathbf{B}}$ are system operators corresponding to observables that depend on the phase space coordinates \mathbf{r}, \mathbf{p} of the probed low-dimensional system (the ‘‘molecule’’). For simplicity, we assume that the system has three degrees of freedom and that the solvent contains n atoms with coordinates \mathbf{R} and \mathbf{P} , such that $d = 3(n + 1)$. We focus on the momentum correlation function of the system, whose time integral determines the diffusion constant of the molecule. It is straightforward to show in this case that the nonexponential part of the correlation function has the form

$$\Lambda_{\mathbf{p}, \mathbf{p}}(\mathbf{r}_0, \mathbf{p}_0, \mathbf{r}_1, \dots, \mathbf{r}_N, \mathbf{R}_0, \mathbf{P}_0, \mathbf{R}_1, \dots, \mathbf{R}_N) = \left[1 + \frac{3}{2}(n + 1) \right] \xi(\mathbf{r}_0, \mathbf{p}_0, \mathbf{r}_N) - 2\gamma_{\text{sol}} \xi(\mathbf{r}_0, \mathbf{p}_0, \mathbf{r}_N) \times \sum_{j=1}^{3d} f_j^*(R_{j,0}, P_{j,0}, R_{j,1}) f_j(R_{j,0}, P_{j,0}, R_{j,N}) - 2\gamma_{\text{mol}} \sum_{j=1}^3 f_j^*(r_{j,0}, p_{j,0}, r_{j,1}) \times \left(-i\hbar \frac{m_{\text{mol}}}{m_{\text{mol}} + \hbar^2 \Delta\beta\gamma_{\text{mol}}} p_j(t) + \xi(\mathbf{r}_0, \mathbf{p}_0, \mathbf{r}_N) f_j(r_{j,0}, p_{j,0}, r_{j,N}) \right) \quad (2.10)$$

where

$$\xi(\mathbf{r}_0, \mathbf{p}_0, \mathbf{r}_N) = \sum_{j=1}^3 w_j(r_{j,0}, p_{j,0}, r_{j,N}) p_j(t) \quad (2.11)$$

$$f_j(x_{j,0}, p_{j,0}, x_{j,k}) = \frac{m_j}{m_j + \hbar^2 \Delta\beta\gamma_j} (x_{j,k} - x_{j,0} + i\hbar \frac{\Delta\beta}{2m} p_{j,0}) \quad (2.12)$$

$$w_j(x_{j,0}, p_{j,0}, x_{j,k}) = \frac{m_j}{m + \hbar^2 \Delta\beta\gamma_j} [p_{j,0} + 2i\hbar\gamma(x_{j,k} - x_{j,0})] \quad (2.13)$$

Unlike in the case of a neat fluid, where the statistics can be enhanced by averaging the observable property of interest with respect to all particles, the calculation of molecular properties in a solvent cannot benefit from such averaging. This implies that FBSD simulations of a molecule in solution will be considerably more demanding. We follow two steps to address this computational challenge: (i) we use grid-based methods to perform the solute integrations, and (ii) we reformulate the FBSD expression in a form suitable for application of IGNoR. Both of these techniques are combined in the procedure described in the next section.

C. IGNoR-Enhanced Solution FBSD. The IGNoR methodology leads to accelerated convergence of a Monte Carlo calculation in the case of moderately oscillatory functions.⁵⁴ The basic idea in this approach is the possibility of relating the negative volume of the oscillatory part to the positive volume through an available exact relation, thus canceling statistical error. The IGNoR technique is applicable to integrals of the type

$$J = \int F(\mathbf{x}) G(\mathbf{x}) d\mathbf{x} \quad (2.14)$$

where F is an oscillatory function whose exact integral

$$I = \int F(\mathbf{x}) d\mathbf{x} \quad (2.15)$$

is known, and G is a smooth function of the integration variables. It is assumed that both functions are real-valued. Complex-valued integrands are treated by separating the product into its real and imaginary parts. Consider the volumes of the positive and negative parts of this function,

$$I^+ = \int F(\mathbf{x}) h(F(\mathbf{x})) d\mathbf{x}, \quad I^- = \int F(\mathbf{x}) h(-F(\mathbf{x})) d\mathbf{x} \quad (2.16)$$

(where h is the Heaviside step function), and their Monte Carlo estimates $\langle I^+ \rangle$ and $\langle I^- \rangle$. From this and the exact value of the integral of F , one can define a ‘‘corrected’’ value of the negative volume,

$$\tilde{I}^- \equiv I - \langle I^+ \rangle \quad (2.17)$$

We also define the integrals

$$J^+ = \int F(\mathbf{x}) G(\mathbf{x}) h(F(\mathbf{x})) d\mathbf{x} \quad \text{and} \quad J^- = \int F(\mathbf{x}) G(\mathbf{x}) h(-F(\mathbf{x})) d\mathbf{x} \quad (2.18)$$

of the product function FG within the positive and negative domains of F . The Monte Carlo estimates $\langle J^+ \rangle$ and $\langle J^- \rangle$ of these integrals are obtained from the same Metropolis random walk performed to calculate the corresponding integrals of F and the ratios

$$\kappa^+ = \frac{\langle J^+ \rangle}{\langle I^+ \rangle} \quad \text{and} \quad \kappa^- = \frac{\langle J^- \rangle}{\langle I^- \rangle} \quad (2.19)$$

are then computed. These ratios describe how much (and in which direction) the factor $g(x)$ modifies the volumes of the positive and negative domains of f . This procedure of calculating the integrals I^+ and J^+ from the same Monte Carlo samples implies that the corresponding estimates $\langle J^+ \rangle$ and $\langle I^+ \rangle$ are correlated, leading to a reduction of statistical uncertainty in their

ratio. IGNoR proceeds by replacing the Monte Carlo estimate of J^- by the corrected estimate

$$\tilde{J}^- \equiv \kappa^- \tilde{I}^- \quad (2.20)$$

Thus, the IGNoR prescription for estimating the desired integral is

$$J \approx \langle J_+ \rangle + \tilde{J}_- = \langle J_+ \rangle - \kappa_- (I - \langle I_- \rangle) \quad (2.21)$$

To apply the IGNoR methodology to the FBSD expression for the correlation function of a molecule in solution, we partition the calculation into two domains, one that contains the degrees of freedom of the solvent and one that includes the coordinates of the molecule in the potential field induced by the solvent. Accordingly, the potential is split into two terms

$$V(\mathbf{r}, \mathbf{R}) = V_{\text{sol}}(\mathbf{R}) + V_{\text{mol-sol}}(\mathbf{r}, \mathbf{R}) \quad (2.22)$$

that contain the solvent-solvent and molecule-solvent interactions, respectively, and the FBSD expression for the momentum correlation function is written in the form

$$C_{\mathbf{p}, \mathbf{p}}(t) = (2\pi\hbar)^{-3(n+1)} \int d\mathbf{r}_0 \int d\mathbf{p}_0 \int d\mathbf{r}_1 \cdots \int d\mathbf{r}_N \int d\mathbf{R}_0 \times \int d\mathbf{P}_0 \int d\mathbf{R}_1 \cdots \int d\mathbf{R}_N \Theta_{\text{sol}}(\mathbf{R}_0, \mathbf{P}_0, \mathbf{R}_1, \dots, \mathbf{R}_N) \times \Theta_{\text{mol-sol}}(\mathbf{r}_0, \mathbf{p}_0, \mathbf{r}_1, \dots, \mathbf{r}_N; \mathbf{R}_0, \mathbf{R}_1, \dots, \mathbf{R}_N) \times \Lambda_{\mathbf{p}, \mathbf{p}}(\mathbf{r}_0, \mathbf{p}_0, \mathbf{r}_1, \dots, \mathbf{r}_N; \mathbf{R}_0, \mathbf{P}_0, \mathbf{R}_1, \dots, \mathbf{R}_N) \quad (2.23)$$

where

$$\Theta_{\text{sol}}(\mathbf{R}_0, \mathbf{P}_0, \mathbf{R}_1, \dots, \mathbf{R}_N) = (2\pi\hbar)^{-3n} \langle \mathbf{R}_0, \mathbf{P}_0 | e^{-\Delta\beta\hat{T}_{\text{sol}}/2} | \mathbf{R}_1 \rangle e^{-\Delta\beta V_{\text{sol}}(\mathbf{R}_1)} \cdots e^{-\Delta\beta V_{\text{sol}}(\mathbf{R}_N)} \langle \mathbf{R}_N | e^{-\Delta\beta\hat{T}_{\text{sol}}/2} | \mathbf{R}_0, \mathbf{P}_0 \rangle \quad (2.24)$$

and

$$\Theta_{\text{mol-sol}}(\mathbf{r}_0, \mathbf{p}_0, \mathbf{r}_1, \dots, \mathbf{r}_N; \mathbf{R}_0, \mathbf{R}_1, \dots, \mathbf{R}_N) = (2\pi\hbar)^{-3} \langle \mathbf{r}_0, \mathbf{p}_0 | e^{-\Delta\beta\hat{T}_{\text{mol}}/2} | \mathbf{r}_1 \rangle e^{-\Delta\beta V_{\text{mol-sol}}(\mathbf{r}_1, \mathbf{R}_1)} \cdots \langle \mathbf{r}_N | e^{-\Delta\beta\hat{T}_{\text{mol}}/2} | \mathbf{r}_0, \mathbf{p}_0 \rangle \quad (2.25)$$

It is easy to see that

$$\int d\mathbf{R}_0 \int d\mathbf{P}_0 \int d\mathbf{R}_1 \cdots \int d\mathbf{R}_N \Theta_{\text{sol}}(\mathbf{R}_0, \mathbf{P}_0, \mathbf{R}_1, \dots, \mathbf{R}_N) = \text{Tr} e^{-\Delta\beta\hat{T}_{\text{sol}}/2} e^{-\Delta\beta\hat{V}_{\text{sol}}} e^{-\Delta\beta\hat{T}_{\text{sol}}} \cdots e^{-\Delta\beta\hat{V}_{\text{sol}}} e^{-\Delta\beta\hat{T}_{\text{sol}}/2} = Z_{\text{sol}} \quad (2.26)$$

that is, the Θ_{sol} part integrates to the partition function of the pure solvent. On the other hand, integrals over the space of the low-dimensional system (which depend parametrically on the solvent) can be performed by quadrature techniques and should be weakly dependent on the solvent coordinates.

To proceed, we divide the integrand of the correlation function into two parts by partitioning eq 2.10 into two terms, Λ_1 and Λ_2 , which comprise the solute and solvent parts, respectively:

$$\Lambda_1(\mathbf{r}_0, \mathbf{p}_0, \mathbf{r}_1, \mathbf{r}_N) = \frac{5}{2} \xi(\mathbf{r}_0, \mathbf{p}_0, \mathbf{r}_N) - 2\gamma_{\text{mol}} \sum_{j=1}^3 f_j^*(r_{j,0}, p_{j,0}, r_{j,1}) \times \left(-i\hbar \frac{m_{\text{mol}}}{m_{\text{mol}} + \hbar^2 \Delta\beta\gamma_{\text{mol}}} p_j(t) + \xi(\mathbf{r}_0, \mathbf{p}_0, \mathbf{r}_N) f_j(r_{j,0}, p_{j,0}, r_{j,N}) \right) \quad (2.27)$$

$$\Lambda_2 = \left[\frac{3}{2} - 2\gamma_{\text{sol}} \sum_{j=1}^{3d} f_j^*(R_{j,0}, P_{j,0}, R_{j,1}) f_j(R_{j,0}, P_{j,0}, R_{j,N}) \right] \xi(\mathbf{r}_0, \mathbf{p}_0, \mathbf{r}_N) \quad (2.28)$$

This partitioning is necessary because of the IGNoR criterion that the G function be smooth in the phase space of the IGNoR integral. Since some components of expression 2.10 are strongly solvent-dependent, the partitioning allows us to shift these into the F portion of the IGNoR integrand. Below, we describe the IGNoR procedure for evaluating the integrals that correspond to each of these two terms.

To obtain the first part of the correlation function, we define

$$F_1(\mathbf{R}_0, \mathbf{P}_0, \mathbf{R}_1, \dots, \mathbf{R}_N) = \Theta_{\text{sol}}(\mathbf{R}_0, \mathbf{P}_0, \mathbf{R}_1, \dots, \mathbf{R}_N) \quad (2.29)$$

and

$$G_1(\mathbf{R}_0, \mathbf{R}_1, \dots, \mathbf{R}_N) = \int d\mathbf{r}_0 \int d\mathbf{p}_0 \int d\mathbf{r}_1 \cdots \int d\mathbf{r}_N \times \Theta_{\text{mol-sol}}(\mathbf{r}_0, \mathbf{p}_0, \mathbf{r}_1, \dots, \mathbf{r}_N; \mathbf{R}_0, \mathbf{R}_1, \dots, \mathbf{R}_N) \Lambda_1(\mathbf{r}_0, \mathbf{p}_0, \mathbf{r}_1, \mathbf{r}_N) \quad (2.30)$$

It is not hard to see that eq 2.30 is the FBSD expression for the (un-normalized) momentum correlation function of the solute in the potential field created by the solvent atoms in the instantaneous configuration specified by the solvent coordinates $\mathbf{R}_0, \mathbf{R}_1, \dots, \mathbf{R}_N$. As such, G_1 is expected to be a slowly varying function of its variables. Evaluation of eq 2.30 is possible by quadrature techniques, for example, by the iterative split operator methodology.⁵⁹

In terms of the functions defined in eqs 2.29 and 2.30, the first part of the desired correlation function becomes

$$C_1(t) = \int d\mathbf{R}_0 \int d\mathbf{P}_0 \int d\mathbf{R}_1 \cdots \int d\mathbf{R}_N \times F_1(\mathbf{R}_0, \mathbf{P}_0, \mathbf{R}_1, \dots, \mathbf{R}_N) G_1(\mathbf{R}_0, \mathbf{R}_1, \dots, \mathbf{R}_N) \quad (2.31)$$

This is exactly in a form suitable for IGNoR, and the various integrals required are obtained via a standard Metropolis random walk using the sampling function

$$\rho(\mathbf{R}_0, \mathbf{P}_0, \mathbf{R}_1, \dots, \mathbf{R}_N) = |\Theta(\mathbf{R}_0, \mathbf{P}_0, \mathbf{R}_1, \dots, \mathbf{R}_N)| \quad (2.32)$$

which is not normalized to unity. Thus, the raw Monte Carlo estimates of the various integrals must be multiplied by the integral of the sampling function. Jezek and Makri have shown⁸ that this integral takes the form

$$\int d\mathbf{R}_0 \int d\mathbf{P}_0 \int d\mathbf{R}_1 \cdots \int d\mathbf{R}_N \rho(\mathbf{R}_0, \mathbf{P}_0, \mathbf{R}_1, \dots, \mathbf{R}_N) = \lambda Z_{\text{sol}} \quad (2.33)$$

where λ is proportional to an integral that is evaluated by straightforward Monte Carlo techniques. Using eq 2.21 and the integral of F_1 given in eq 2.29, the IGNoR estimate of eq 2.31 is

$$C_1(t) = \frac{Z_{\text{sol}}}{Z} [\lambda \langle J_1^+ \rangle_{\rho_{\text{norm}}} - \kappa_1^- + \kappa_1^- \lambda \langle I_1^+ \rangle_{\rho_{\text{norm}}}] \quad (2.34)$$

where $\langle J_1^+ \rangle_{\rho_{\text{norm}}}$ and $\langle I_1^+ \rangle_{\rho_{\text{norm}}}$ denote the Monte Carlo estimates with respect to a *normalized* sampling function of the integrals of F_1 and $F_1 G_1$, respectively, over the domain where F_1 is positive.

For the calculation of the second term of the time correlation function, we define

$$F_2(\mathbf{R}_0, \mathbf{P}_0, \mathbf{R}_1, \dots, \mathbf{R}_N) = \Theta_{\text{sol}}(\mathbf{R}_0, \mathbf{P}_0, \mathbf{R}_1, \dots, \mathbf{R}_N) \times \left[\frac{3}{2} - n - 2\gamma_{\text{sol}} \sum_{j=1}^{3d} f_j^*(R_{j,0}, P_{j,0}, R_{j,1}) f_j(R_{j,0}, P_{j,0}, R_{j,N}) \right] \quad (2.35)$$

and

$$G_2(\mathbf{R}_0, \mathbf{R}_1, \dots, \mathbf{R}_N) = \int d\mathbf{r}_0 \int d\mathbf{p}_0 \int d\mathbf{r}_1 \cdots \int d\mathbf{r}_N \times \Theta_{\text{mol-sol}}(\mathbf{r}_0, \mathbf{p}_0, \mathbf{r}_1, \dots, \mathbf{r}_N; \mathbf{R}_0, \mathbf{R}_1, \dots, \mathbf{R}_N) \xi(\mathbf{r}_0, \mathbf{p}_0, \mathbf{r}_N) \quad (2.36)$$

Then the second term of the correlation function has the form

$$C_2(t) = \int d\mathbf{R}_0 \int d\mathbf{P}_0 \int d\mathbf{R}_1 \cdots \int d\mathbf{R}_N F_2 \times (\mathbf{R}_0, \mathbf{P}_0, \mathbf{R}_1, \dots, \mathbf{R}_N) G_2(\mathbf{R}_0, \mathbf{R}_1, \dots, \mathbf{R}_N) \quad (2.37)$$

It is easy to show that eq 2.35 is closely related to the FBSD integrand of a correlation function where the operators \hat{A} and \hat{B} are equal to the identity operator in the space of the solvent particles,

$$\text{Tr}_{\text{sol}} [e^{-\beta \hat{H}_{\text{sol}}} \hat{1} e^{i\hat{H}_{\text{sol}}t/\hbar} \hat{1} e^{-i\hat{H}_{\text{sol}}t/\hbar}] = (2\pi\hbar)^{-3n} \int d\mathbf{R}_0 \int d\mathbf{P}_0 \int d\mathbf{R}_1 \cdots \int d\mathbf{R}_N \Theta_{\text{sol}}(\mathbf{R}_0, \mathbf{P}_0, \mathbf{R}_1, \dots, \mathbf{R}_N) \times \left[\left(\frac{3}{2} - n \right) - 2\gamma_{\text{sol}} \sum_{j=1}^{3d} f_j^*(R_{j,0}, P_{j,0}, R_{j,1}) f_j(R_{j,0}, P_{j,0}, R_{j,N}) \right] \quad (2.38)$$

It follows that the integral of eq 2.35 vanishes. The function G_2 is again evaluated by iterative techniques at each value of the solvent coordinates.

The IGNoR evaluation of this term proceeds similarly to that described previously. Again, using eq 2.32 as the sampling function and noting that $I_2 = 0$, as argued in the preceding paragraph, we find

$$C_2(t) = \frac{Z_{\text{sol}}}{Z} [\lambda \langle J_2^+ \rangle_{\rho_{\text{norm}}} - \kappa_1^- + \kappa_2^- \lambda \langle I_2^+ \rangle_{\rho_{\text{norm}}}] \quad (2.39)$$

The desired correlation function is obtained by adding eqs 2.34 and 2.39. One observes that the resulting correlation function contains the ratio of the solvent partition function to the partition function of the molecule-solvent system as a common factor. Partition functions can be computed by appropriate path integral Monte Carlo (PIMC) techniques, but such a calculation is not necessary in the present case. This is so because the common factor Z_{sol}/Z is independent of time and thus amounts to an overall scaling of the obtained time function. As was pointed out in a recent paper, it is easy to scale the entire correlation function, that is, the values of

$$\lambda \langle J_1^+ \rangle_{\rho_{\text{norm}}} - \kappa_1^- + \kappa_1^- \lambda \langle I_1^+ \rangle_{\rho_{\text{norm}}} + \lambda \langle J_2^+ \rangle_{\rho_{\text{norm}}} - \kappa_2^- + \kappa_2^- \lambda \langle I_2^+ \rangle_{\rho_{\text{norm}}} \quad (2.40)$$

at the desired time points, to the value of the momentum correlation function at zero time (which equals the kinetic energy of the molecule-solvent system) that is readily available through a PIMC calculation.

To summarize the procedure described so far, one performs a Monte Carlo random walk in the space of the solvent variables $\mathbf{R}_0, \mathbf{P}_0, \mathbf{R}_1, \dots, \mathbf{R}_N$ to estimate the particular integrals that enter the IGNoR prescription for each of the two terms in the correlation

function. At each solvent configuration, the functions G_1 and G_2 are computed via iterative grid methods. (Because these functions depend only mildly on the solvent coordinates, it is not necessary in practice to calculate them each time a distant solvent particle is moved; we find that these functions need to be updated only once per few Monte Carlo steps for those solvent particles in the immediate neighborhood of the solute, and less frequently when solute particles outside the first solvation shell are moved.)

D. Repartitioned IGNoR-Enhanced FBSD. Finally, we describe here a strategy for improving the Monte Carlo statistics even further, at least for the short-time values of the correlation function. We repartition the integrands of each of the two parts of the correlation function, defining new functions F'_i that include the zero-time value of G_i ($i = 1, 2$), while the new functions G'_i consist of the value of G_i relative to its initial value:

$$F'_i = F_i G_i(t=0), \quad G'_i(t) = \frac{G_i(t)}{G_i(t=0)} \quad (2.41)$$

Implementation of the IGNoR procedure is still possible because the new F'_i function integrates to the exact kinetic energy of the solute-solvent system, which is available with high precision through a PIMC calculation. Because $G'_i(t=0) = 1$, the Monte Carlo error of this procedure at $t = 0$ is very small, equal to that attained by the PIMC calculation of the kinetic energy. As time increases, the statistical error grows, becoming, at worst, comparable to that obtained through the non-repartitioned procedure detailed in the previous subsection. As the trajectories corresponding to various solvent configurations evolve in time, the rescaled solute integral $G'_i(t)$ deviates from unity and becomes less smooth, leading to an increase in the statistical error, which is likely to approach the typical IGNoR error within one period of oscillation of the correlation function.

III. Numerical Test

We illustrate the procedure described in section II by calculating the momentum autocorrelation function for a solute particle in a model one-dimensional solvent. The solute has the mass of a Ne atom, while the solvent particles are 15 times heavier. The solute and solvent particles are arranged in a line. The interaction between any pair of atoms, as well as all atom-wall interactions, are described by a Lennard-Jones potential

$$V(r) = 4\epsilon \left[\left(\frac{\sigma}{r} \right)^{12} - \left(\frac{\sigma}{r} \right)^6 \right] \quad (2.42)$$

with $\sigma = 2\text{\AA}$ and $\epsilon = 20 \text{ cm}^{-1}$. The solute is a single particle initially positioned in such a way that an equal number of solvent particles are on either side of it, while the solvent consists of n atoms where $n = 2, 6, \text{ or } 8$. In order to avoid singularities in the evaluated potential in the integration over the solute phase space, the solvent sampling function inserts an additional Lennard-Jones "phantom" particle halfway between the two walls, thus effectively preventing the solvent particles from crowding the space that would ultimately be used for the integration over the solute degrees of freedom. We report numerical results at a temperature $T = 39.5 \text{ K}$ using $N = 3$ path integral beads for each particle.

The momentum autocorrelation (scaled to its zero-time value) of the solute particle interacting with 6 or 8 solvent particles is depicted in Figures 1 and 2. The procedure for calculating error bars in the IGNoR-enhanced results is summarized in the Appendix. Figure 1 compares the IGNoR-enhanced FBSD result

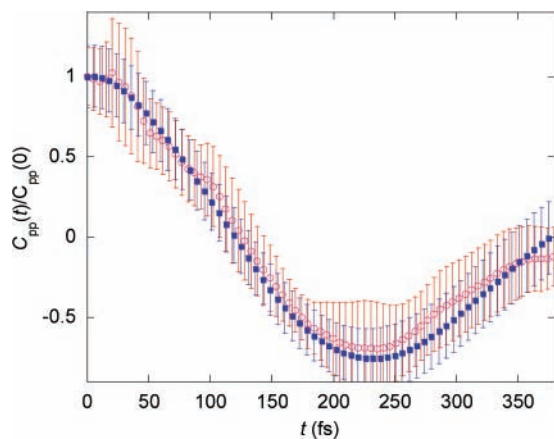


Figure 1. Real parts of the solute momentum autocorrelation function for the model described in section III with six solvent particles. Red: results obtained via a direct application of the FBSD methodology (eq 2.6), with 1.2 million Monte Carlo points per dimension. Blue: results obtained through the IGNUr-enhanced FBSD methodology with 35 000 Monte Carlo points per dimension.

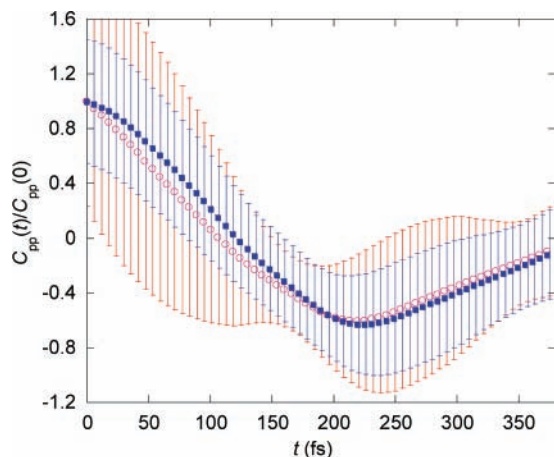


Figure 2. Comparison of solution FBSD results with (blue) and without (red) IGNUr improvement for the case of eight solvent particles. The parameters are the same as in Figure 1.

obtained from a calculation that used 35 000 Monte Carlo passes per integral dimension, to the result of a direct FBSD calculation of the same quantity (i.e., a direct implementation of eq 2.23) that used 1.2×10^6 Monte Carlo passes per integration variable. (We do not present the raw Monte Carlo results with 35 000 passes, as the corresponding error bars are approximately 6 times larger and cannot be drawn on the same scale.) Calculations were performed on a 20-processor Linux cluster, and the CPU times required for the two calculations were roughly equivalent. Even though the IGNUr-enhanced FBSD procedure used about 35 times fewer samples than the conventional Monte Carlo calculation, the error bars of the former are actually slightly smaller than those of the latter. This dramatic reduction of statistical error demonstrates the benefits attainable by the methodology described in this paper. Of course, the grid-based calculation of the solute integrals makes the IGNUr-enhanced FBSD calculation more expensive for each Monte Carlo point, but this increase in CPU cost should become relatively less significant when the number of solvent particles is large.

Figure 2 presents a similar calculation, now with the solute in an environment of eight solvent particles. The comparison is now to a solution-FBSD result (i.e., the sum of eqs 2.31 and 2.37 evaluated by Monte Carlo, with the G_i functions obtained via the iterative grid technique) to which no IGNUr error enhancement has been applied. Both calculations were

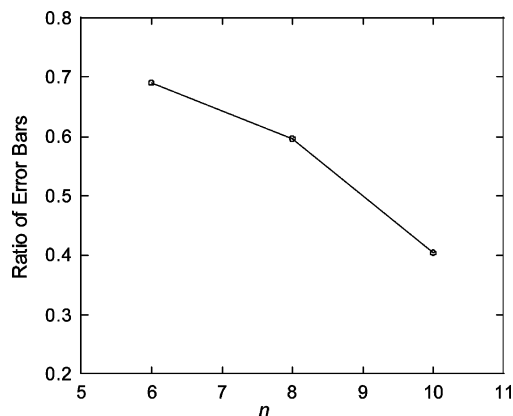


Figure 3. Ratio of statistical errors in IGNUr-enhanced FBSD and plain solution FBSD results as a function of the number of solvent particles.

performed with the same 35 000 Monte Carlo passes per dimension. It is seen that performing the solute integrals by quadrature leads to a large reduction of statistical error compared to the raw Monte Carlo treatment of all coordinates. (The error bars of the raw Monte Carlo results with 35 000 passes are 6 times larger than those shown in Figure 1.) Further, the additional reduction of statistical error achieved through application of the IGNUr procedure is seen to be significant.

Finally, Figure 3 illustrates the reduction of statistical error achieved by the IGNUr methodology as a function of system size. Plotted is the ratio of the IGNUr-enhanced FBSD result and the solution-FBSD result (where the solute integrations are performed by quadrature methods) for different numbers of particles, with a fixed number (35 000) of Monte Carlo points per integral dimension. As we suggest in our discussion of the IGNUr procedure, the improvement over standard estimates is most significant in cases when the G function (in our case, the solute integral) is weakly dependent on the variables of integration. As more particles are added to the solvent farther away from the solute particle, the corresponding weak solute-solvent interaction leads to a weak dependence of the G functions on the coordinates of those particles. As a result, the IGNUr error grows very slowly with the number of solvent particles, in contrast to the uncorrected result whose statistical uncertainty increases at an exponential rate.

IV. Concluding Remarks

In this paper we have extended the FBSD methodology to a particle in solution. We have derived an FBSD expression for the momentum correlation function of the solute and discussed some potentially challenging issues associated with its numerical evaluation. Namely, if the Boltzmann operator of the solvent particles needs to be quantized by more than a single path integral “bead”, the oscillatory character of the integral leads to poor statistics as the number of solvent particles increases. Because such calculations are typically done with a single solute particle in the simulation cell, one cannot take advantage of averaging, as in the case of a neat fluid.

The first step in the direction of addressing these challenges involves partitioning the FBSD integrand into solvent and solute domains and performing the solute integrals by quadrature-based methods. As shown in Figure 2, this treatment leads to a significant reduction in the statistical error. The second (and perhaps more crucial step for application to real systems with hundreds of particles) involves the expression of the solution-FBSD correlation function in a form amenable to IGNUr. This

procedure exploits knowledge of the exact integral in the absence of the solute particles to achieve a partial cancellation of error. The improvement attained this way becomes more dramatic as the number of solvent atoms is increased.

Even though the IGNoR methodology was applied here to the special case of a molecule in solution, we believe it will find application in many different situations where integrals of oscillatory functions must be calculated using Monte Carlo techniques. Many quantities of interest in quantum dynamics and statistical mechanics involve an oscillatory function that comprises the integrand of a known quantity, such as a partition function or a related observable that is available either analytically or through an easier (thus very accurate) numerical calculation. Knowledge of such an integral is exploited in IGNoR, leading to a substantial cancellation of statistical error.

Acknowledgment. This material is based upon work supported by the National Science Foundation under Award CHE 05-18452. The calculations were performed on a Linux cluster acquired through NSF CRIF 05-41659.

Appendix

Here we summarize our procedure for obtaining Monte Carlo error bars within the IGNoR methodology,

$$J \approx (\langle \kappa^+ \rangle - \langle \kappa^- \rangle) \langle I^+ \rangle + \langle \kappa^- \rangle I \quad (\text{A.1})$$

where the quantities in brackets denote Monte Carlo estimates. The sources of error in the IGNoR estimate emanate from the statistical error in the integral ratios κ^+ and κ^- , as well as the error in the estimate of the positive volume of the oscillatory part of the integrand, I^+ .

Using the principles of error propagation, the statistical uncertainty of the ratio κ^+ can be obtained from the following expression:

$$\sigma_{\kappa^+}^2 = \left\{ \left(\frac{\sigma_{J^+}}{\langle J^+ \rangle} \right)^2 + \left(\frac{\sigma_{I^+}}{\langle I^+ \rangle} \right)^2 - \frac{2 \text{cov}(J^+, I^+)}{\langle J^+ \rangle \langle I^+ \rangle} \right\} \kappa_+^2 \quad (\text{A.2})$$

(where $\text{cov}(J^+, I^+)$ indicates the covariance of these integrals). A similar calculation gives the statistical error for κ^- . Applying the laws of error propagation to eq A.1, we arrive at the following expression for the overall error estimate of the J integral computed by IGNoR:

$$\sigma_J^2 = \sigma_{\kappa^+ - \kappa^-}^2 + \sigma_{I^+}^2 + \sigma_{I^-}^2 \quad (\text{A.3})$$

where

$$\sigma_{\kappa^+ - \kappa^-}^2 = \sigma_{\kappa^+}^2 + \sigma_{\kappa^-}^2 - 2 \text{cov}(\kappa^+, \kappa^-) \quad (\text{A.4})$$

In the case of a smooth G function, the error in the ratios κ^\pm will be lowered appreciably relative to the error obtained with a raw Monte Carlo estimate of J by virtue of the covariance term in expression A.2. For example, in the limit where G is constant, the error in these ratios will vanish. Thus, a sufficiently precise estimate of the desired integral can be obtained with a number of Monte Carlo samples that may be too small for the raw estimate of the integral to be meaningful.

The covariance that leads to the lowering of the ratio errors, expression A.2, must be computed from estimates of I^+ and J^+ obtained from the same random walk. However, it is not necessary to use that estimate of I^+ to obtain the IGNoR estimate in expression A.1; given that, in many cases, the calculation of this integral is very inexpensive, one can obtain a more accurate

estimate of I^+ by conducting a second, longer random walk (which also lowers its error estimate). In the case of solution FBSD discussed in this paper, this longer random walk to obtain I^+ requires very little additional cost, since this integral does not require trajectory propagation or the calculation of solute averages via split propagator methods. The calculations reported in section III took advantage of this procedure for further reduction of statistical error.

In cases of complex F and G , their product yields four terms, two of which are real. Thus, the procedure for obtaining the IGNoR error involves repeating the procedure described above for each of the four products.

References and Notes

- (1) Makri, N.; Thompson, K. *Chem. Phys. Lett.* **1998**, *291*, 101.
- (2) Thompson, K.; Makri, N. *J. Chem. Phys.* **1999**, *110*, 1343.
- (3) Thompson, K.; Makri, N. *Phys. Rev. E* **1999**, *59*, R4729.
- (4) Shao, J.; Makri, N. *J. Phys. Chem. A* **1999**, *103*, 7753.
- (5) Shao, J.; Makri, N. *J. Phys. Chem. A* **1999**, *103*, 9479.
- (6) Kuhn, O.; Makri, N. *J. Phys. Chem.* **1999**, *103*, 9487.
- (7) Shao, J.; Makri, N. *J. Chem. Phys.* **2000**, *113*, 3681.
- (8) Jezek, E.; Makri, N. *J. Phys. Chem.* **2001**, *105*, 2851.
- (9) Makri, N. In *Fluctuating Paths and Fields*; Janke, W., Pelster, A., Schmidt, H.-J., Bachmann, M., Eds.; World Scientific: Singapore, 2001.
- (10) Wright, N. J.; Makri, N. *J. Chem. Phys.* **2003**, *119*, 1634.
- (11) Makri, N. *J. Phys. Chem. B* **2002**, *106*, 8390.
- (12) Nakayama, A.; Makri, N. *J. Chem. Phys.* **2003**, *119*, 8592.
- (13) Wright, N. J.; Makri, N. *J. Phys. Chem. B* **2004**, *108*, 6816.
- (14) Nakayama, A.; Makri, N. *Chem. Phys.* **2004**, *304*, 147.
- (15) Makri, N.; Nakayama, A.; Wright, N. *J. Theor. Comput. Chem.* **2004**, *3*, 391.
- (16) Nakayama, A.; Makri, N. *Proc. Natl. Acad. Sci. U.S.A.* **2005**, *102*, 4230.
- (17) Liu, J.; Makri, N. *Chem. Phys.* **2006**, *322*, 23.
- (18) Liu, J.; Makri, N. *Mol. Phys.* **2006**, *104*, 1267.
- (19) Kegerreis, J.; Makri, N. *J. Comput. Chem.* **2007**, *28*, 818.
- (20) Van Vleck, J. H. *Proc. Natl. Acad. Sci. U.S.A.* **1928**, *14*, 178.
- (21) Herman, M. F.; Kluk, E. *Chem. Phys.* **1984**, *91*, 27.
- (22) Miller, W. H. *J. Chem. Phys.* **1970**, *53*, 3578.
- (23) Miller, W. H. *Adv. Chem. Phys.* **1974**, *25*, 69.
- (24) Kay, K. G. *J. Chem. Phys.* **1994**, *100*, 4432.
- (25) Kay, K. *J. Chem. Phys.* **1997**, *107*, 2313.
- (26) Thoss, M.; Miller, W. H.; Stock, G. *J. Chem. Phys.* **2000**, *112*, 10282.
- (27) Guallar, V.; Batista, V. S.; Miller, W. H. *J. Chem. Phys.* **2000**, *113*, 9510.
- (28) Pollak, E.; Shao, J. *J. Phys. Chem. A* **2003**, *107*, 7112.
- (29) Zhang, S.; Pollak, E. *J. Chem. Phys.* **2003**, *119*, 11058.
- (30) Sun, X.; Wang, H.; Miller, W. H. *J. Chem. Phys.* **1998**, *109*, 4190.
- (31) Thoss, M.; Wang, H.; Miller, W. H. *J. Chem. Phys.* **2001**, *114*, 9220.
- (32) Wigner, E. *J. Chem. Phys.* **1937**, *5*, 720.
- (33) Brown, R. C.; Heller, E. J. *J. Chem. Phys.* **1981**, *75*, 186.
- (34) Sun, X.; Wang, H.; Miller, W. H. *J. Chem. Phys.* **1998**, *109*, 7064.
- (35) Wang, H.; Sun, X.; Miller, W. H. *J. Chem. Phys.* **1998**, *108*, 9726.
- (36) Pollak, E.; Liao, J.-L. *J. Chem. Phys.* **1998**, *108*, 2733.
- (37) Miller, W. H. *J. Phys. Chem.* **1999**, *103*, 9384.
- (38) Miller, W. H. *Faraday Discuss.* **1998**, *110*, 1.
- (39) Sun, X.; Miller, W. H. *J. Chem. Phys.* **1999**, *110*, 6635.
- (40) Wang, H.; Thoss, M.; Miller, W. H. *J. Chem. Phys.* **2000**, *112*, 47.
- (41) Gelabert, R.; Gimenez, X.; Thoss, M.; Wang, H.; Miller, W. H. *J. Chem. Phys.* **2001**, *114*, 2572.
- (42) Wang, H.; Thoss, M.; Sorge, K. L.; Gelabert, R.; Gimenez, X.; Miller, W. H. *J. Chem. Phys.* **2001**, *114*, 2562.
- (43) Skinner, D. E.; Miller, W. H. *J. Chem. Phys.* **1999**, *111*, 10787.
- (44) Ovchinnikov, M.; Apkarian, V. A.; Voth, G. A. *J. Chem. Phys.* **2001**, *114*, 7130.
- (45) Martin-Fierro, E.; Pollak, E. *J. Chem. Phys.* **2006**, *125*, 164104.
- (46) Shi, Q.; Geva, E. *J. Phys. Chem. A* **2003**, *107*, 9059.
- (47) Shi, Q.; Geva, E. *J. Phys. Chem. A* **2003**, *107*, 9070.
- (48) Frantsuzov, P. A.; Mandelshtam, V. A. *J. Chem. Phys.* **2004**, *121*, 9247.
- (49) Liu, J.; Miller, W. H. *J. Chem. Phys.* **2006**, *125*, 224104.
- (50) Marinica, D. C.; Gaigeot, M. P.; Borgis, D. *Chem. Phys. Lett.* **2006**, *423*, 390.
- (51) Shao, J.; Pollak, E. *J. Chem. Phys.* **2006**, *125*, 133502.
- (52) Lawrence, C. P.; Nakayama, A.; Makri, N.; Skinner, J. L. *J. Chem. Phys.* **2004**, *120*, 6621.
- (53) Makri, N. *J. Phys. Chem.* **1993**, *97*, 2417.

- (54) Makri, N. *Chem. Phys. Lett.* **2004**, 400, 446.
- (55) Makri, N.; Shao, J. In *Accurate Description of Low-Lying Electronic States and Potential Energy Surfaces*; Hoffmann, M, Ed.; Oxford University Press: New York, 2002.
- (56) Chandler, D.; Wolynes, P. G. *J. Chem. Phys.* **1981**, 74, 4078.
- (57) Ceperley, D. M.; Mitas, L. *Adv. Chem. Phys.* **1996**, 93, 1.
- (58) Feynman, R. P. *Statistical Mechanics*; Addison-Wesley: Redwood City, CA, 1972.
- (59) Feit, M. D.; Fleck, J. A. J.; Steiger, A. *J. Comput. Phys.* **1982**, 47, 412.